

The fine structure of Gowdy spacetimes

David Garfinkle

Dept. of Physics, University of Guelph, Guelph, Ontario, N1G 2W1, Canada

E-mail: david@physics.uoguelph.ca

Abstract. The approach to the singularity in Gowdy spacetimes consists of velocity term dominated behavior, except at a set of isolated points. At and near these points, spiky features grow. This paper reviews what is known about these spikes.

1. Introduction

There have been several investigations, both analytical and numerical, of the approach to the singularity in inhomogeneous cosmologies.[1]-[14] The most extensively studied class of these spacetimes is the class of Gowdy spacetimes[15] on $T^3 \times R$. Theorems due to Isenberg and Moncrief[1] showed that the polarized Gowdy spacetimes are asymptotically velocity term dominated (AVTD). It was then natural to ask whether this is also true of the more general unpolarized Gowdy spacetimes. This was a more difficult question since the relevant equations are linear in the polarized case but nonlinear in the unpolarized case. To address this question, Berger and Moncrief[5] performed numerical simulations of the approach to the singularity in Gowdy spacetimes. They obtained the following curious result: the behavior is AVTD except at a set of isolated points. At and near these exceptional points, features appear that grow ever steeper and narrower as the singularity is approached. Berger and Moncrief referred to these features as “spiky features,” though for brevity we will simply call them “spikes.” These spikes form a “fine structure” on the simpler and more prevalent behavior of the rest of the spacetime.

The purpose of this paper is to review what is known about these spikes. Section 2 presents the basic equations governing the Gowdy spacetimes on $T^3 \times R$. The next three sections concern a variety of methods and results, with numerical methods and results presented in section 3, analytical approximations in section 4 and mathematical results in section 5. Conclusions are given in section 6.

2. Equations

The Gowdy metric on $T^3 \times R$ takes the form

$$ds^2 = e^{\lambda/2} t^{-1/2} (-dt^2 + dx^2) + t[e^P(dy + Qdz)^2 + e^{-P}dz^2] \quad (1)$$

where P, Q and λ are functions of t and x . The T^3 spatial topology is imposed by having $0 \leq x, y, z \leq 2\pi$ and having P, Q and λ be periodic functions of x . The vacuum Einstein field equations split into “evolution” equations for P and Q

$$P_{,tt} + t^{-1}P_{,t} - P_{,xx} + e^{2P}(Q_{,x}^2 - Q_{,t}^2) = 0 \quad (2)$$

$$Q_{,tt} + t^{-1}Q_{,t} - Q_{,xx} + 2(P_{,t}Q_{,t} - P_{,x}Q_{,x}) = 0 \quad (3)$$

and “constraint” equations for λ

$$\lambda_{,t} = t[P_{,t}^2 + P_{,x}^2 + e^{2P}(Q_{,t}^2 + Q_{,x}^2)] \quad (4)$$

$$\lambda_{,x} = 2t(P_{,x}P_{,t} + e^{2P}Q_{,x}Q_{,t}) \quad (5)$$

(here $_{,a} = \partial/\partial a$). The constraint equations determine λ once P and Q are known. The integrability conditions for the constraint equations are satisfied as a consequence of the evolution equations. Since the evolution equations do not depend on λ there is essentially a complete decoupling of constraints from evolution equations. Therefore, for the purposes of this paper we will treat only equations (2-3). The only restriction that the constraints place on initial data for equations (2-3) is the following: since λ at

$x = 0$ is the same as λ at $x = 2\pi$, it follows that the integral from 0 to 2π of the right hand side of equation (5) must vanish. We require that this restriction is satisfied by the initial data for equations (2-3) and then these equations insure that the restriction is also satisfied at subsequent times.

The singularity is at $t = 0$. It is often helpful to introduce the coordinate $\tau \equiv -\ln t$. Thus the singularity is approached as $\tau \rightarrow \infty$. In terms of this coordinate, the evolution equations (2-3) become

$$P_{,\tau\tau} - e^{2P}Q_{,\tau}^2 - e^{-2\tau}P_{,xx} + e^{2(P-\tau)}Q_{,x}^2 = 0 \quad (6)$$

$$Q_{,\tau\tau} + 2P_{,\tau}Q_{,\tau} - e^{-2\tau}(Q_{,xx} + 2P_{,x}Q_{,x}) = 0 \quad (7)$$

Equations (6-7) are the equations of motion corresponding to the Hamiltonian $H = H_K + H_V$ where

$$H_K = \frac{1}{2} \int_0^{2\pi} dx (\pi_P^2 + e^{-2P} \pi_Q^2), \quad (8)$$

$$H_V = \frac{1}{2} e^{-2\tau} \int_0^{2\pi} dx (P_{,x}^2 + e^{2P} Q_{,x}^2). \quad (9)$$

One can also put the evolution equations (2-3) in characteristic form: define null coordinates $\xi \equiv t + x$ and $\eta \equiv t - x$ and characteristic variables A, B, C and D given by

$$A = (\xi + \eta)P_{,\eta}, \quad (10)$$

$$B = (\xi + \eta)P_{,\xi}, \quad (11)$$

$$C = (\xi + \eta)e^P Q_{,\eta}, \quad (12)$$

$$D = (\xi + \eta)e^P Q_{,\xi}. \quad (13)$$

Then equations (2-3) become

$$A_{,\xi} = (\xi + \eta)^{-1} [CD + (A - B)/2] \quad (14)$$

$$B_{,\eta} = (\xi + \eta)^{-1} [CD + (B - A)/2] \quad (15)$$

$$C_{,\xi} = (\xi + \eta)^{-1} [-AD + (C - D)/2] \quad (16)$$

$$D_{,\eta} = (\xi + \eta)^{-1} [-BC + (D - C)/2] \quad (17)$$

As we will see in the next section, each of these different ways of writing the evolution equations has its uses for numerical simulations.

3. Numerical methods and results

We now consider numerical simulations of the evolution equations for P and Q . Since we wish to examine the behavior as the singularity is approached, it is most convenient to simulate equations (6-7) and examine the behavior for large τ . One simple numerical method is to use centered differences for spatial derivatives and the iterated Crank-Nicholson (ICN) method[16] for time evolution. (Spikes were first found[5] using the symplectic method to be described below. However, the ICN method has been used[17] to simulate Gowdy spacetimes with spatial topology $S^2 \times S^1$). The ICN method is in the class of so called ‘‘predictor-corrector’’ methods: first taking a crude approximation

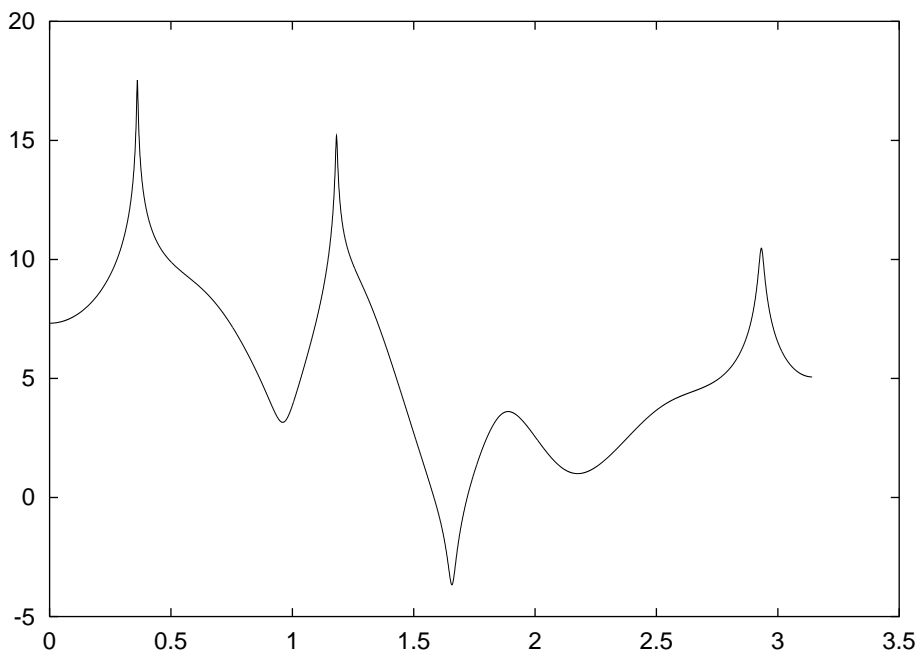


Figure 1. Plot of P vs x for $v_0 = 5$ at $\tau = 10$. Here $0 \leq x \leq \pi$

to the evolution and then refining it. The symplectic method is in the class of “operator splitting” methods: splitting the equations of motion into two pieces, each of which is evolved separately. Here centered differences means that for a quantity F at spatial grid point i we have $F_{,x} \rightarrow (F_{i+1} - F_{i-1})/(2\Delta x)$ and $F_{,xx} \rightarrow (F_{i+1} + F_{i-1} - 2F_i)/(\Delta x)^2$. The ICN method is the following: we put the equations in the form $S_{,\tau} = W$ (*i.e.* first order in time) by making $P_{,\tau}$ and $Q_{,\tau}$ extra variables. Then we evolve the variables S from time step n to time step $n + 1$ using

$$S^{n+1} = S^n + \frac{\Delta\tau}{2}[W(S^n) + W(S^{n+1})] \quad (18)$$

We choose S^n as our initial guess for S^{n+1} and use this guess in the right hand side of equation (18) to produce a better guess. This process is iterated 3 times to evolve to the next time step.

We wish to consider small scale structure generated by the approach to the singularity. For that reason we choose initial data that itself has as little small scale structure as possible. Following references[5, 6] we use the data $P = 0$, $P_{,\tau} = v_0 \cos x$, $Q = \cos x$, $Q_{,\tau} = 0$ at time $\tau = 0$. (Here v_0 is a constant). As argued in reference[6] the type of fine structure generated by this family of initial data should be generic. Figures (1) and (2) show the evolution to $\tau = 10$ of these data for $v_0 = 5$.

From these plots it is apparent that there are narrow upward pointing features in P at $x \approx 0.36$, $x \approx 1.2$ and $x \approx 2.9$. In addition, there is a narrow downward pointing feature in P at $x \approx 1.66$ which coincides with the location of a narrow feature in Q . For reasons that will become apparent in section 5, we adopt the notation of reference[11] and call the upward pointing features in P “true spikes” and the downward pointing

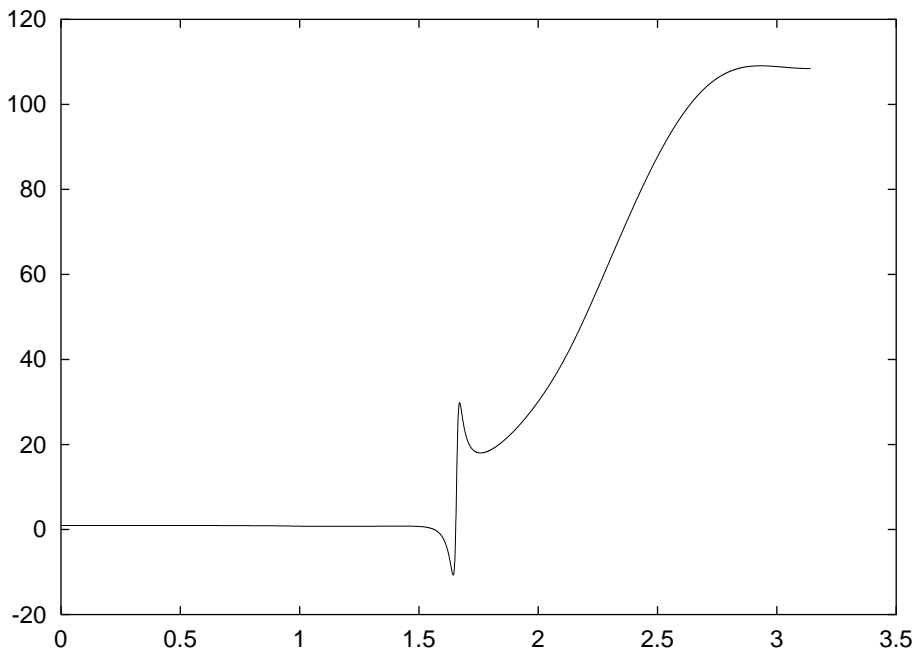


Figure 2. Plot of Q vs x for $v_0 = 5$ at $\tau = 10$. Here $0 \leq x \leq \pi$

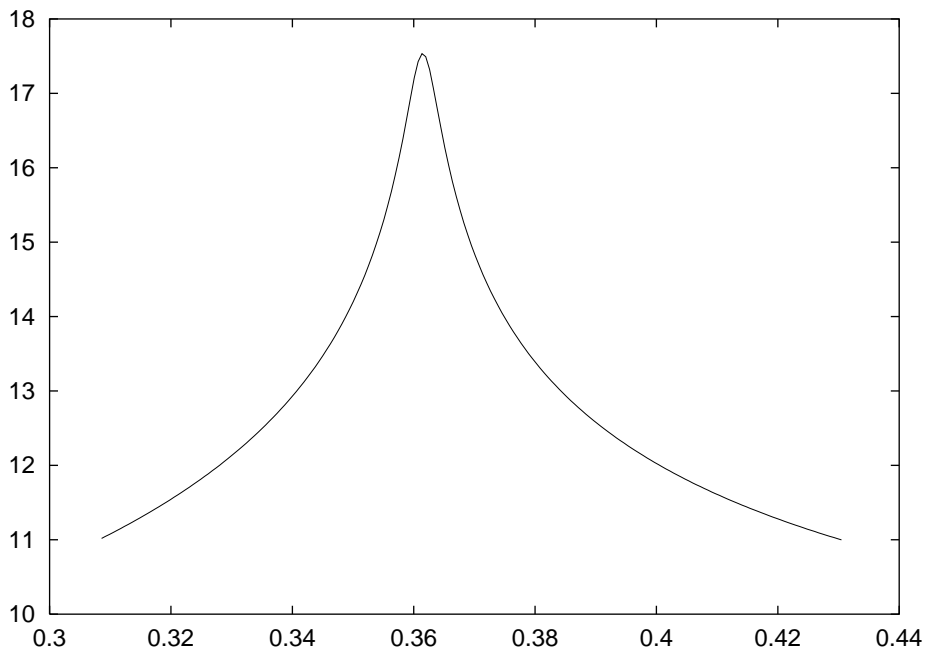


Figure 3. Plot of P vs x for $v_0 = 5$ at $\tau = 10$. This is a closer look at the true spike at $x \approx 0.36$

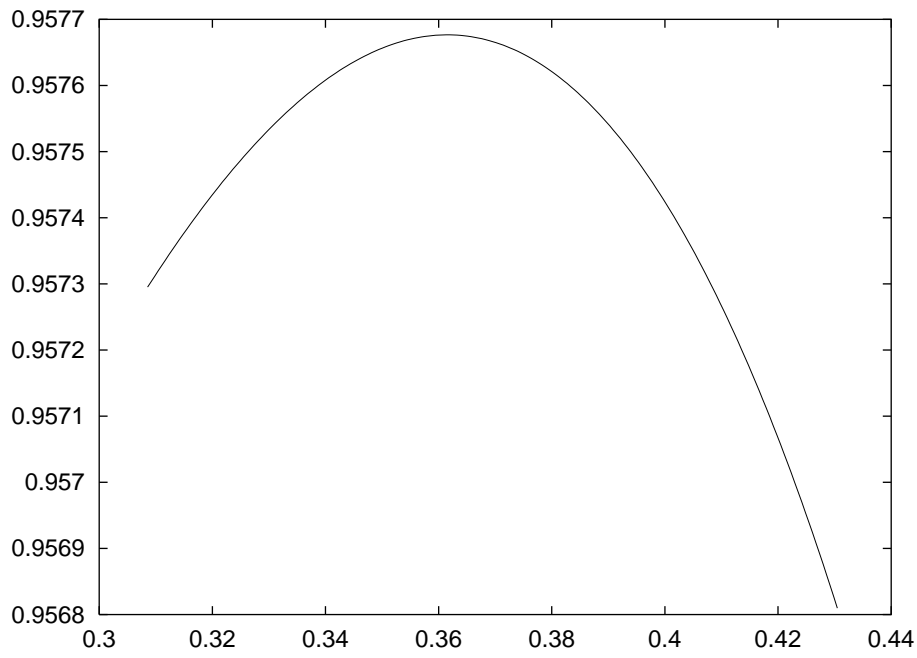


Figure 4. Plot of Q vs x for $v_0 = 5$ at $\tau = 10$. This is a closer look at the true spike at $x \approx 0.36$

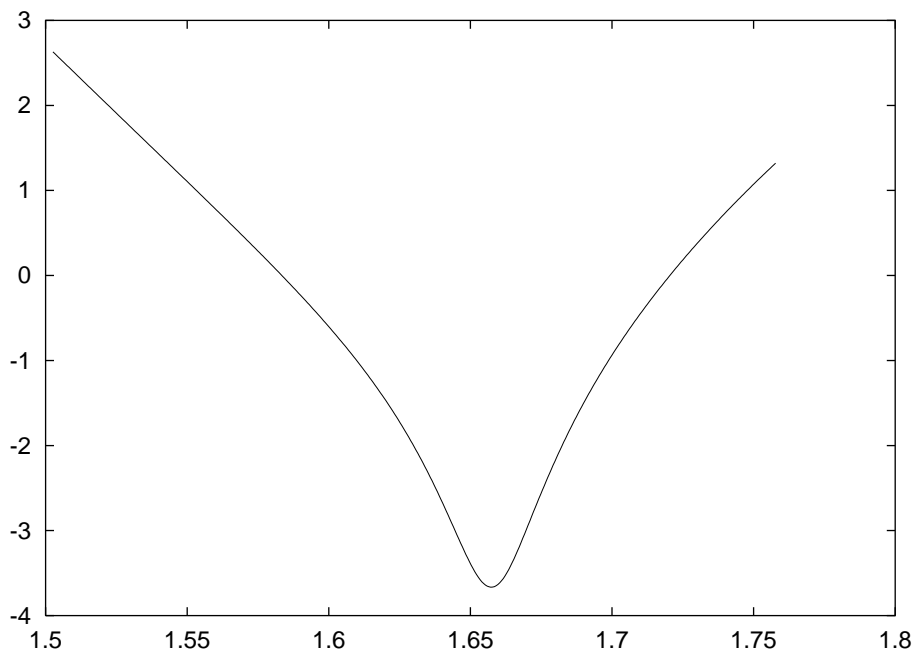


Figure 5. Plot of P vs x for $v_0 = 5$ at $\tau = 10$. This is a closer look at the false spike

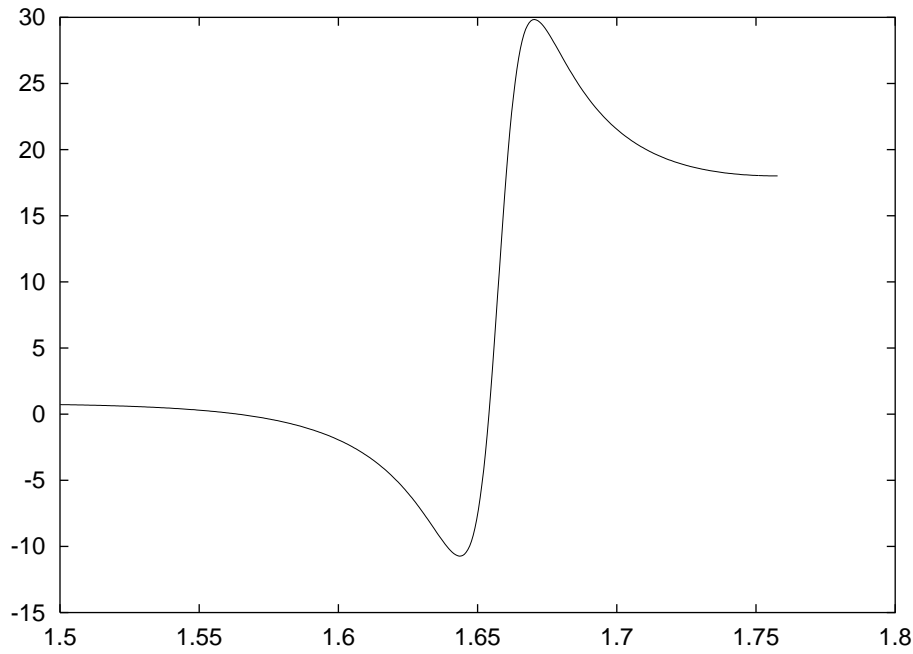


Figure 6. Plot of Q vs x for $v_0 = 5$ at $\tau = 10$. This is a closer look at the false spike

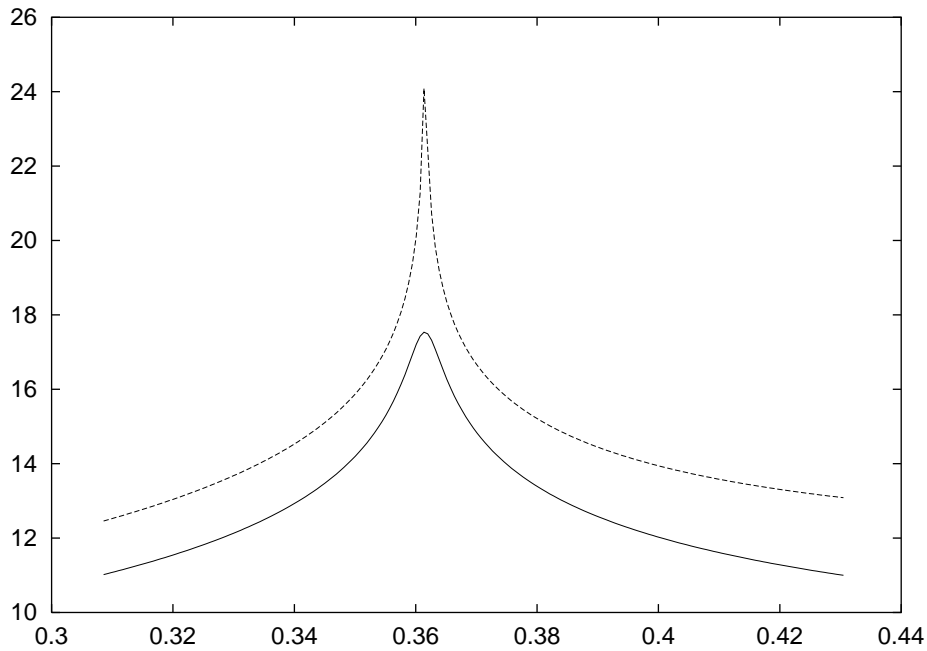


Figure 7. Plot of P vs x for $v_0 = 5$ at $\tau = 10$ (solid line) and $\tau = 15$ (dashed line). This is a close look at the true spike at two different times. Note that the spike is higher and more narrow at the later time.

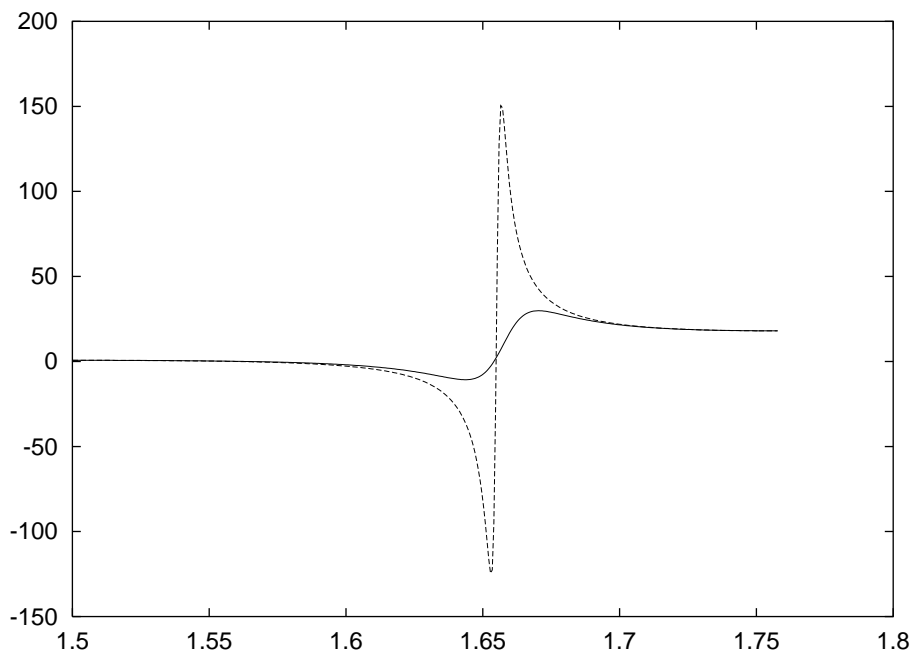


Figure 8. Plot of Q vs x for $v_0 = 5$ at $\tau = 10$ (solid line) and $\tau = 15$ (dashed line). This is a close look at the false spike at two different times. Note that the spike is higher and more narrow at the later time.

features in P along with narrow feature in Q a “false spike.”

Figures (3) and (4) provide a closer look at the true spike at $x \approx 0.36$ while figures (5) and (6) do the same for the false spike. Note that Q has an extremum at the position of the true spike.

The spikes become steeper and narrower as the singularity is approached. Figure (7) shows P at the true spike at $x \approx 0.36$ at $\tau = 10$ and $\tau = 15$. Figure (8) shows Q at the false spike at $\tau = 10$ and $\tau = 15$.

The ICN method that we have described is second order accurate. However, one might want higher order accuracy, and this is provided by the symplectic methods used in[5]. The symplectic method[18] works as follows: begin with a system whose equations of motion come from a Hamiltonian of the form $H = H_K + H_V$ where the sub-hamiltonians H_K and H_V each correspond to a system that can be solved in closed form. (Note that this condition is satisfied by the Gowdy evolution equations (6-7) where the corresponding sub-hamiltonians are given in equations (8-9)). Let $\mathcal{U}_K(\Delta\tau)$ be the evolution operator that corresponds to evolving the system with Hamiltonian H_K for a time $\Delta\tau$. Correspondingly define $\mathcal{U}_V(\Delta\tau)$. Now consider the operator $\mathcal{U}_{(2)}(\Delta\tau)$ defined by

$$\mathcal{U}_{(2)}(\Delta\tau) = \mathcal{U}_K(\Delta\tau/2)\mathcal{U}_V(\Delta\tau)\mathcal{U}_K(\Delta\tau/2). \quad (19)$$

In words, $\mathcal{U}_{(2)}(\Delta\tau)$ evolves using H_K for half a time step, then using H_V for a full time step and then using H_K for half a time step. One can show[18] that $\mathcal{U}_{(2)}$ is a second order accurate operator for the full system described by $H = H_K + H_V$. Furthermore,

using $\mathcal{U}_{(2)}$ one can construct evolution operators of any accuracy one wishes. The fourth order accurate operator $\mathcal{U}_{(4)}$ is given by

$$\mathcal{U}_{(4)}(\Delta\tau) = \mathcal{U}_{(2)}(s\Delta\tau)\mathcal{U}_{(2)}[(1-2s)\Delta\tau]\mathcal{U}_{(2)}(s\Delta\tau) \quad (20)$$

where $s = 1/(2 - 2^{1/3})$. The general n th order accurate operator $\mathcal{U}_{(n)}$ is built recursively from lower order $\mathcal{U}_{(n)}$ in similar ways.

To take advantage of n th order accuracy in time, the codes must also have n th order accuracy in space. Thus the second order accurate centered differences must be replaced by more complicated finite differences that are n th order accurate. There is another advantage besides higher order accuracy in using the symplectic method to study the approach to the singularity: as the singularity is approached, H_V appears to become small compared to H_K . If H_V were completely negligible, then the operator $\mathcal{U}_{(2)}$ (and therefore $\mathcal{U}_{(4)}$ and all higher order $\mathcal{U}_{(n)}$) would be exact. Thus as the singularity is approached, the symplectic method may be even more accurate than one might guess from the formal order of accuracy. (This fact has been used in simulations of Mixmaster spacetimes[19].)

A numerical method will be accurate only if there are enough spatial points to resolve all features. However, the spikes grow ever narrower; thus for any fixed resolution there will come a time when that resolution is not sufficient to resolve the spikes. Indeed the simulations of [5, 6] are often run so long that some spikes are not resolved; however it is argued in[6] that this does not affect the accuracy of the simulation in regions away from the spikes.

To resolve the spikes for a long time, it is better to use a grid that does not have a fixed resolution. One way to do this is to use the technique of adaptive mesh refinement (AMR).[20] This technique adds extra mesh points in places where the existing mesh is not sufficiently fine to resolve the features. AMR was applied to the Gowdy spacetimes by Hern and Stewart.[21] Unfortunately, AMR codes are quite involved and difficult to write. Moreover, the full machinery of AMR may not be needed since it appears that in a given Gowdy spacetime there is a limited number of spikes and that their positions change very little as the singularity is approached. One can then construct a mesh that is finer in the places where one knows the spikes will be.[22]

Alternatively, one can study a single spike using a characteristic method.[23] Here, the initial data surface is an outgoing light ray and one evolves along ingoing light rays. One can choose the last grid point to correspond to the light ray that hits the center of the spike at the singularity. As a consequence of this choice, the grid shrinks as the evolution proceeds in such a way that the grid is always of an appropriate size to resolve the spike.

4. Analytical approximations

We now turn to analytical approximations to the equations of motion (6-7). Our treatment closely follows that of[6]. One obvious approximation is the following: since

the approach to the singularity is $\tau \rightarrow \infty$, it is natural to neglect terms in equations (6-7) proportional to $e^{-2\tau}$. Dropping such terms results in the following equations:

$$P_{,\tau\tau} - e^{2P} Q_{,\tau}^2 = 0, \quad (21)$$

$$Q_{,\tau\tau} + 2P_{,\tau} Q_{,\tau} = 0 \quad (22)$$

These equations are called the velocity term dominated (VTD) equations. (Note that the VTD equations are the equations of motion corresponding to the sub-hamiltonian H_K). A solution of equations (6-7) is called asymptotically velocity term dominated (AVTD) if there is a solution of the VTD equations that it approaches as $\tau \rightarrow \infty$.

The VTD equations can be solved in closed form with the general solution given by

$$P = p + \ln[\cosh v\tau + \cos \psi \sinh v\tau], \quad (23)$$

$$Q = q + \frac{e^{-p} \sin \psi \tanh v\tau}{1 + \cos \psi \tanh v\tau}. \quad (24)$$

Here $v \geq 0$ and the quantities p , q , v and ψ are functions of x . The behavior of the false spikes follows from equations (23-24). For $\cos \psi \neq -1$ the behavior of these solutions as $\tau \rightarrow \infty$ is $P \rightarrow \bar{p} + v\tau$ and $Q \rightarrow \bar{q}$ where \bar{p} and \bar{q} are functions of x given by $\bar{p} = p + \ln[(1 + \cos \psi)/2]$ and $\bar{q} = q + e^{-p} \sin \psi / (1 + \cos \psi)$. Let x_1 be a point where $\cos \psi = -1$. Then clearly there is some steep behavior near x_1 . Let a subscript 1 denote the value of the function at x_1 and let ψ_1' denote $\psi_{,x}$ at x_1 . Then near x_1 and for large τ it follows from equations (23- 24) that

$$P \approx p_1 - v_1\tau + \ln[1 + (\psi_1')^2 e^{2v_1\tau} (x - x_1)^2 / 4] \quad (25)$$

$$Q \approx q_1 - \frac{e^{-p_1} \psi_1'(x - x_1)}{2e^{-2v_1\tau} + (\psi_1')^2 (x - x_1)^2 / 2} \quad (26)$$

Equations (25-26) provide an analytic approximation to the behavior of false spikes. Figures (9-10) show the behavior of P and Q respectively for these formulas. Here $p_1 = 5$, $q_1 = 0$, $v_1 = 0.5$, $x_1 = 0$, $\psi_1' = 1$ and $\tau = 10$.

To treat the behavior of the true spikes, we first consider the validity of the VTD approximation by using the ‘‘method of consistent potentials’’ (MCP).[4] That is, we assume the large τ behavior $P \rightarrow \bar{p} + v\tau$, $Q \rightarrow \bar{q}$ and see whether the terms in equations (6 -7) that we have neglected are in fact negligible. The term $e^{2(P-\tau)} Q_{,x}^2$ has behavior $e^{2[\bar{p}+(v-1)\tau]} \bar{q}_{,x}^2$. Thus this term is negligible only if $v < 1$. The numerical simulations of [5, 6] show that in fact v evolves to a value less than 1 except at the true spikes. To find an explanation for this behavior we must consider what happens when v is initially greater than 1. We are still justified in using equation (22) which yields $Q_{,\tau} = \pi_Q e^{-2P}$ where π_Q is a function of x . This turns the term $-e^{2P} Q_{,\tau}^2$ in equation (6) into $-e^{-2P} \pi_Q^2$ which can be neglected since P is growing. We can also approximate $Q(\tau, x)$ by $\bar{q}(x)$. Thus we are led to approximate equation (6) by

$$P_{,\tau\tau} + e^{2(P-\tau)} \bar{q}_{,x}^2 = 0. \quad (27)$$

This equation can be solved in closed form to yield

$$P = p + \tau - \ln[\cosh w\tau - \cos \phi \sinh w\tau]. \quad (28)$$

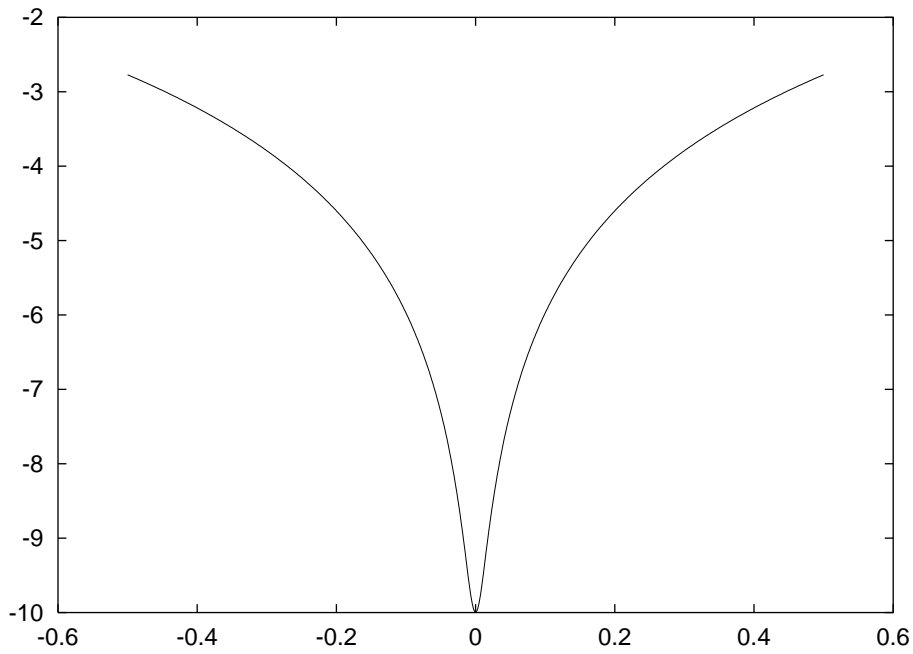


Figure 9. Plot of P vs x for the analytic approximation, equation (25) for a false spike

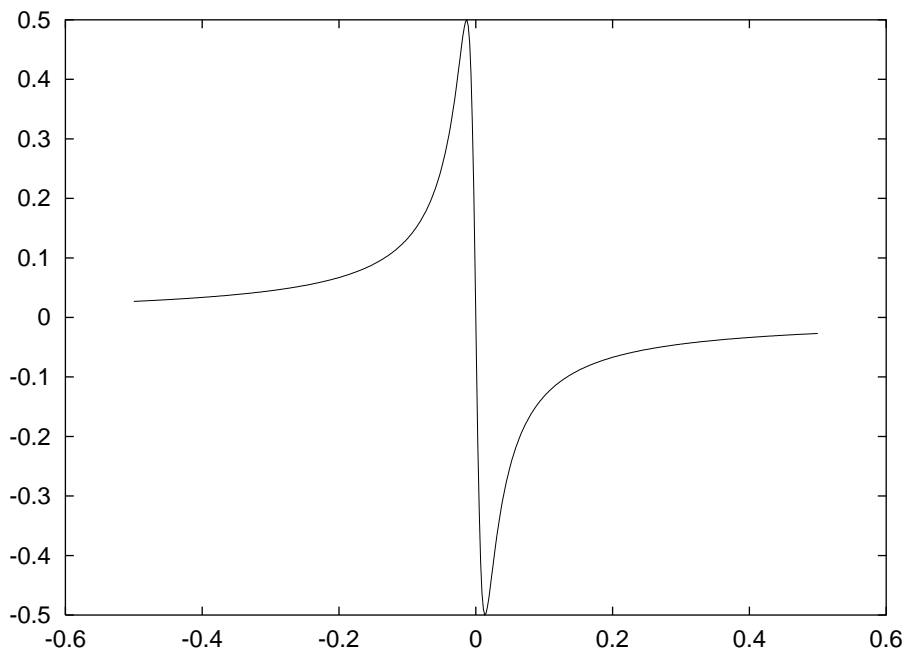


Figure 10. Plot of Q vs x for the analytic approximation, equation (26) for a false spike

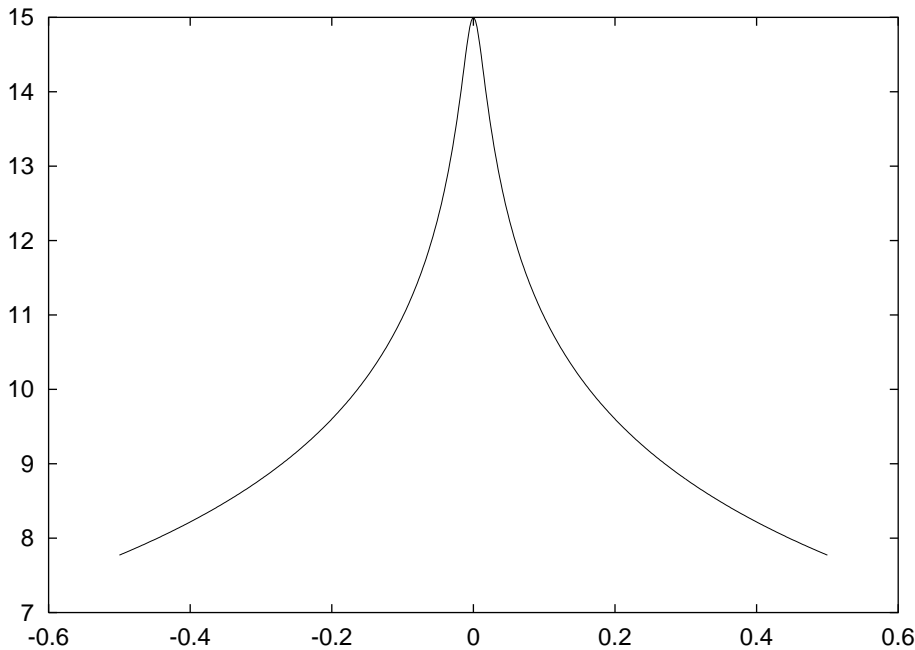


Figure 11. Plot of P vs x for the analytic approximation, equation (29) for a true spike

Here $w > 0$ and p , w and ϕ are functions of x and we have $\bar{q}_{,x} = e^{-p}w \sin \phi$. For $\cos \phi \neq 1$ the large τ behavior of this solution is $P \rightarrow \bar{p} + v\tau$ where $\bar{p} = p - \ln[(1 - \cos \phi)/2]$ and $v = 1 - w$. Let x_2 be a point where $\cos \phi = 1$ and use a subscript 2 to denote the value of the function at x_2 . Then near x_2 and for large τ it follows from equation (28) that

$$P \approx p_2 + (1 + w_2)\tau - \ln[1 + (\phi_2')^2 e^{2w_2\tau} (x - x_2)^2 / 4] \quad (29)$$

Equation (29) provides an analytic approximation to the behavior of true spikes. Figure (11) shows the behavior of P for this formula. Here $p_2 = 0$, $w_2 = 0.5$, $x_2 = 0$, $\phi_2' = 1$ and $\tau = 10$.

The dynamics of spike formation can be understood as follows: Define the “potentials” $V_1 = \pi_Q^2 e^{-2P}$ and $V_2 = e^{2(P-\tau)} Q_{,x}^2$. Then the behavior of P can be regarded as the the dynamics of a particle in these potentials. If $P_{,\tau} < 0$ then a “bounce” off of V_1 will give rise to a transition $P_{,\tau} \rightarrow -P_{,\tau}$ which will make $P_{,\tau}$ positive. If $P_{,\tau} > 1$ then a bounce off of V_2 will give rise to a transition $P_{,\tau} \rightarrow 1 - P_{,\tau}$ and thus $P_{,\tau} < 1$. Eventually, after a finite number of bounces $P_{,\tau}$ will be in the range $0 < P_{,\tau} < 1$. This occurs provided that both potentials V_1 and V_2 are nonvanishing. At a point x_1 where $V_1 = 0$ a false spike can form since $P_{,\tau} < 0$ is allowed. At a point x_2 where $V_2 = 0$ a true spike can form since $P_{,\tau} > 1$ is allowed.

We now consider the validity of the approximation (29). Using the MCP we find that the term $e^{-2\tau} P_{,xx}$ goes as $e^{2(w-1)\tau}$. This term is thus negligible provided that $w < 1$ or equivalently that $P_{,\tau}$ at the center of the spike is less than 2. This leaves open the question of what happens to “high velocity” spikes, *i.e.* those for which $P_{,\tau}$ at the center of the spike is initially larger than 2. This question was answered recently in the

numerical work of [23]. The simulations of [23] show that initially high velocity spikes are forced by the term $e^{-2\tau}P_{,xx}$ to lower velocity. In the end, either the spike itself disappears or the velocity at the center of the spike is brought to the range $1 < P_{,\tau} < 2$.

5. Mathematical results

Here we consider two mathematical questions about spikes: (1) are spikes geometrical features or coordinate artifacts? and (2) to what extent are solutions with spikes rigorously proven to exist? This section is essentially a summary of the results of [11]. The reader should see that work and references therein for a more detailed treatment.

So far we have presented the spikes in terms of the behavior of P and Q as functions of τ and x . That is, we have considered the coordinate dependence of metric components. One might then wonder whether the spikes are simply artifacts of the coordinate system in which the metric (1) is expressed. However, the Gowdy coordinates and metric components themselves have geometric meaning in terms of the symmetries of the spacetime. The coordinate t is defined by the area of each symmetry T^2 being $4\pi^2 t$. The coordinate x is the harmonic function conjugate to t (see Chapter 3, problem 2 of [24]). The vector fields $(\partial/\partial y)^a$ and $(\partial/\partial z)^a$ are Killing fields. Furthermore, P and Q can be expressed in terms of inner products of Killing fields. Nonetheless, there is a restricted coordinate freedom that preserves this relation between coordinates and geometry. In particular, consider the transformation that simply switches the coordinates y and z . This leaves the metric in the form of (1) but changes the pair (P, Q) to (\tilde{P}, \tilde{Q}) given by

$$e^{-\tilde{P}} = \frac{e^{-P}}{Q^2 + e^{-2P}}, \tag{30}$$

$$\tilde{Q} = \frac{Q}{Q^2 + e^{-2P}}. \tag{31}$$

Following [11] we will use the notation $(\tilde{P}, \tilde{Q}) = I(P, Q)$ where the ‘‘I’’ is for inversion. Now suppose that (P, Q) is a solution of the VTD equations without spikes and which therefore has the large τ behavior $P \rightarrow \bar{p} + v\tau$ and $Q \rightarrow \bar{q}$. Then \tilde{Q} has the large τ behavior

$$\tilde{Q} \rightarrow \frac{\bar{q}}{\bar{q}^2 + e^{-2\bar{p}}e^{-2v\tau}}. \tag{32}$$

Therefore \tilde{Q} has a false spike at points where \bar{q} vanishes. Thus false spikes are not geometric quantities since they can be made to appear and disappear by a coordinate transformation.

In contrast true spikes can be shown to be true geometric objects. This is done by examining the behavior of curvature invariants at the spikes as the singularity is approached. The asymptotic behavior of curvature invariants as the singularity is approached is different at a true spike than at nearby points.

We now turn to a different type of transformation that takes a solution (P, Q) of equations (6-7) and produces a solution (\bar{P}, \bar{Q}) that represents a different spacetime.

The transformation is given by

$$\bar{P} = \tau - P, \tag{33}$$

$$\bar{Q}_{,\tau} = -e^{2(P-\tau)} Q_{,x}, \tag{34}$$

$$\bar{Q}_{,x} = -e^{2P} Q_{,\tau}. \tag{35}$$

This transformation is essentially the analog for Gowdy spacetimes of the Kramer-Neugebauer transformation[25] for stationary axisymmetric spacetimes. The integrability conditions for equations (34-35) are satisfied as a result of the equations of motion (6-7). Following[11] we will use the notation $(\bar{P}, \bar{Q}) = \text{GE}(P, Q)$. Here the ‘‘GE’’ stands for ‘‘Gowdy to Ernst.’’ For our purposes what is important is that if (P, Q) has a false spike then $\text{GE}(P, Q)$ will have a true spike. Thus from a solution (P, Q) with no spikes at all we can generate a solution $\text{GE}(I(P, Q))$ with true spikes. The problem of proving existence of solutions with spikes has thus been reduced to the problem of proving existence of solutions with no spikes.

How then does one prove existence of solutions with no spikes? Here we simply sketch what is done and refer the reader to [8, 9] for details. At first it might seem that what is needed is a global existence theorem. However, spikes are essentially asymptotic behavior as the singularity is approached. Thus a local existence theorem will suffice provided that it is local in a neighborhood of the singularity. What is needed for such a theorem is to put the equations in Fuchsian form

$$t \frac{\partial \vec{u}}{\partial t} + N(x) \vec{u} = t \vec{f}(t, x, \vec{u}, \vec{u}_{,x}) \tag{36}$$

for a system described by the vector valued function \vec{u} . One needs certain properties for the function \vec{f} and matrix N . Using these properties, one proves that there exists a solution in a neighborhood of $t = 0$ and with $\vec{u} = 0$ at $t = 0$. To write the Gowdy equations in Fuchsian form, one must first correctly guess (based on equations (23-24)) functions that have the $t \rightarrow 0$ behavior of P and Q . One then writes P and Q as these functions plus remainder terms. One then rewrites the Gowdy evolution equations (2-3) as a Fuchsian system for the remainder terms. In this way existence of P and Q with the appropriate asymptotic behavior is proved. The P and Q obtained in this way do not have spikes. However, applying the transformations I and GE to this P and Q one obtains a rigorous proof of existence of Gowdy spacetimes with spikes.

6. Conclusions

When spikes were first found by Berger and Moncrief[5] they seemed quite mysterious. Now, about a decade later, we have a very good understanding of this phenomenon. A variety of numerical simulations have allowed us a close look at the process of spike formation and at the properties of the spikes. Analytical approximations give us an understanding of how the spikes form as well as an approximate description of their shape and time development. Mathematical results have shown that the false spikes

are mere coordinate artifacts while the true spikes are real geometric phenomena. In addition it has been possible to prove rigorously that solutions with spikes exist.

Acknowledgments

The work I have done on this subject has been done in collaboration with Beverly Berger and Marsha Weaver. I would like to thank them as well as Vince Moncrief, Jim Isenberg and Alan Rendall for numerous helpful discussions over the years. This work was supported by NSF grant PHY-9988790 to Oakland University.

References

- [1] Isenberg J and Moncrief V 1990 *Ann. Phys. (N.Y.)* **199** 84
- [2] Chruściel P T, Isenberg J and Moncrief V 1990 *Class. Quantum Grav.* **73** 1671
- [3] Chruściel P T 1991 *Proceedings of the Center for Mathematics and its Applications* **27**
- [4] Grubišić B and Moncrief V 1993 *Phys. Rev.* **D47** 2371
- [5] Berger B K and Moncrief V 1993 *Phys. Rev.* **D48** 4676
- [6] Berger B K and Garfinkle D 1998 *Phys. Rev.* **D57** 4767
- [7] Weaver M, Isenberg J and Berger B K 1998 *Phys. Rev. Lett.* **80** 2984
- [8] Kichenassamy S and Rendall A 1998 *Class. Quantum Grav.* **15** 1339
- [9] Rendall A 2000 *Class. Quantum Grav.* **17** 3305
- [10] Andersson L and Rendall A 2001 *Commun. Math. Phys.* **218** 479
- [11] Rendall A and Weaver M 2001 *Class. Quantum Grav.* **18** 2959
- [12] Berger B K, Isenberg J and Weaver M 2001 *Phys. Rev.* **D64** 084006
- [13] Elst H, Ugla C and Wainwright J 2002 *Class. Quantum Grav.* **19** 51
- [14] Ringström H 2002 *Preprint gr-qc/0204044*
- [15] Gowdy R H 1971 *Phys. Rev. Lett.* **27** 826
- [16] Choptuik M W 1994 *Deterministic Chaos in General Relativity* edited by D. Hobill, A. Burd and A. Coley (Plenum, New York) p 155
- [17] Garfinkle D 1999 *Phys. Rev.* **D60** 104010
- [18] Suzuki M 1990 *Phys. Lett. A* **146** 319
- [19] Berger B K, Garfinkle D and Strasser E 1997 *Class. Quantum Grav.* **14** L29
- [20] Berger M J and Oliger J 1984 *J. Comput. Phys.* **53** 484
- [21] Hern S J and Stewart J M 1998 *Class. Quantum Grav.* **15** 1581
- [22] Weaver M 1999 *PhD Thesis, University of Oregon*
- [23] Garfinkle D and Weaver M 2003 *Phys. Rev.* **D67**, 124009
- [24] Wald R M 1985 *General Relativity* (University of Chicago Press)
- [25] Kramer D and Neugebauer G 1968 *Commun. Math. Phys.* **10** 132